Survey of Ti-, B-, and Y-based soft x-ray–extreme ultraviolet multilayer mirrors for the 2- to 12-nm wavelength region

Claude Montcalm, Patrick A. Kearney, J. M. Slaughter, Brian T. Sullivan, M. Chaker, Henri Pépin, and Charles M. Falco

We have performed an experimental investigation of Ti-, B_4C-, B-, and Y-based multilayer mirrors for the soft x-ray–extreme ultraviolet (XUV) wavelength region between 2.0 and 12.0 nm. Eleven different material pairs were studied: Ti/Ni, Ti/Co, Ti/Cu, Ti/W, B_4C/Pd, B/Mo, Y/Pd, Y/Ag, Y/Mo, Y/Nb, and Y/C. The multilayers were sputter deposited and were characterized with a number of techniques, including low-angle x-ray diffraction and normal incidence XUV reflectometry. Among the Ti-based multilayers the best results were obtained with Ti/W, with peak reflectances up to 5.2% at 2.79 nm at 61° from normal incidence. The B_4C/Pd and B/Mo multilayer mirrors had near-normal incidence (5°) peak reflectances of 11.5% at 8.46 nm and 9.4% at 6.67 nm, respectively, whereas a Y/Mo multilayer mirror had a maximum peak reflectance of 25.6% at 11.30 nm at the same angle. The factors limiting the peak reflectance of these different multilayer mirrors are discussed.

Key words: Soft x ray, extreme ultraviolet, XUV optics, multilayer mirrors, normal incidence reflectance, thin films, interfaces, sputtering, enthalpy, Gibbs free energy of formation, titanium, nickel, cobalt, copper, tungsten, boron, boron-carbide, palladium, molybdenum, yttrium, silver, niobium, carbon.

1. Introduction

Remarkable progress has been made in the field of normal incidence soft x-ray–extreme ultraviolet (XUV) multilayer mirrors.[1,2] For example, many high-reflectance Si/Mo multilayer mirrors for wavelengths between 12.5 and 25.0 nm have been produced over the past decade, including mirrors with peak reflectance $R \approx 66\%$ at $\lambda = 13.4$ nm.[3,4] More recently, Be/Mo multilayer mirrors have proven to be the most effective for wavelengths slightly above 11.2 nm, with a measured normal incidence peak reflectance of 68.7% at $\lambda = 11.3$ nm.[5] At shorter wavelengths the best near-normal incidence peak reflectances reported up to now were achieved with B_4C/Ru, C/Fe and Sc/W multilayer mirrors with 20% at 7.0 nm, 13% at 4.5 nm, and 3.3% at 3.1 nm, respectively.[6–8] A more detailed overview of different multilayer mirrors was presented by Spiller (Ref. 1, p. 175).

There are wavelength regions, however, in which currently none of the well-established material pairs can achieve reflectances that are required for many applications. For example, microscopy in the water window region (2.3 nm $< \lambda <$ 4.4 nm) would permit examination of wet biological cells with a resolution many times that of a visible-light microscope and without the radiation damage of conventional electron microscopes.[9] It would also be advantageous to perform projection lithography in the 8- to 12-nm

When this research was performed, C. Montcalm was with the Institut National de la Recherche Scientifique-Énergie et Materiaux, Université du Québec, P.O. Box 1020, Varennes, Québec J3X 1S2, Canada, and the Institute for Microstructural Sciences, National Research Council of Canada, Montréal Road, Ottawa, Ontario K1A 0R6, Canada, and a visiting researcher at the Laboratory for X-Ray Optics, Optical Sciences Center and Department of Physics, University of Arizona, Tucson, Arizona 85721. J. M. Slaughter, P. A. Kearney, and C. M. Falco were with the Laboratory for X-Ray Optics, Optical Sciences Center and Department of Physics, University of Arizona, Tucson, Arizona 85721. C. Montcalm and P. A. Kearney are now with the Advanced Microtechnology Program, Lawrence Livermore National Laboratory, P.O. Box 808, L-395, Livermore, California 94551. B. T. Sullivan is with the Institute for Microstructural Sciences, National Research Council of Canada, Montréal Road, Ottawa, Ontario K1A 0R6, Canada. M. Chaker and H. Pépin are with the Institut National de la Recherche Scientifique-Énergie et Matériaux, Université du Québec, P.O. Box 1020, Varennes, Québec J3X 1S2, Canada.

Received 23 October 1995; revised manuscript received 22 February 1996.

0003-6935/96/255134-14$10.00/0

wavelength region, where a resolution better than 0.1 μm could be achieved while maintaining a depth of focus larger than ±0.5 μm.[10,11] Other applications involving soft x-ray optics, such as astronomy,[12] x-ray lasers,[13] plasma diagnostics,[14] and spectroscopy[15] also would benefit from better normal incidence mirrors at these shorter wavelengths. The need for new material pairs in the 2- to 12-nm short-wavelength region has motivated the research that is discussed here.

Previous studies have dealt with the material requirements for this wavelength region.[16,17] However, it is useful to review some important aspects that make the fabrication of XUV mirrors more difficult for shorter wavelengths. XUV multilayer mirrors typically consist of a periodic stack of two alternating materials. The material that is less absorbing is known as the spacer, whereas the other material is known as the absorber. The layer thicknesses of these materials are chosen such that the light reflected from each interface adds constructively to give a high reflectance at the wavelength and angle of interest. The thickness of a spacer–absorber bilayer is known as the period thickness of the multilayer.

The ultimate reflectance that can be achieved with a multilayer mirror is limited by the difference in the complex refractive indices of the spacer and absorber materials (i.e., their optical contrast), their extinction coefficients, the number of periods, the layer thickness reproducibility, and the quality of the multilayer interfaces. The goal is to find a material pair with a high optical contrast and minimum absorption and then to fabricate a multilayer with interface imperfections much smaller than the wavelength of interest. However, there are two main reasons why these requirements are increasingly more difficult to satisfy for shorter and shorter wavelengths. First, the complex refractive index of all materials approaches unity with decreasing wavelengths λ, and the reflectance at any interface is therefore proportional to λ^4 in this short-wavelength region (Ref. 1, p. 26). Hence, more periods are needed to achieve a desired reflectance. However, there is a maximum number of periods beyond which the incident light will not penetrate because of the absorption in the layers. Second, as the multilayer period thickness becomes smaller for shorter wavelengths, the interface widths resulting from interface roughness, interdiffusion, or compound formation can be comparable with the layer thicknesses. This is a serious problem because the performance of a mirror decreases drastically when the interface width is greater than ~10% of the layer thickness. It is therefore more crucial to minimize interface imperfections for these shorter-wavelength mirrors compared to the longer-wavelength mirrors.

In Section 2 the selection criteria for choosing the best material pairs for a given wavelength region are reviewed. In addition, the best spacer material candidates for three different wavelength regions (2.8–3.6 nm, 6.7–11.5 nm, and 8.0–12.0 nm) are presented along with a list of suitable absorber materials. The deposition system and conditions used to fabricate XUV multilayers for these three wavelength regions are described in Section 3. The experimental results for each wavelength region are presented in Section 4, and the performance of each material pair is discussed in Section 5. From the analysis of the results, some trends concerning factors that limit the reflectance of XUV multilayer mirrors are highlighted.

2. Material Selection

The best material pairs will be those that form smooth and compositionally abrupt interfaces and that have a high optical contrast and minimal absorption. Hence, it is important to take into account not only the optical properties of the materials but also their physical and chemical properties as well.

The following selection criteria should be used to establish the best material pair candidates: (a) absorption—search for materials that have a low extinction coefficient (k) in a given wavelength region (spacer material); (b) optical contrast—search for materials that have a large difference in n and k with respect to the spacer materials (high interface reflectance); (c) microstructure—select material pairs that are likely to form continuous and smooth layers when deposited; (d) miscibility—select materials pairs with low interdiffusivity and low chemical reactivity, i.e., low miscibility; (e) contamination—select materials that have a low chemical reactivity with common gas species such as oxygen, nitrogen, water vapor, sulfur, and so on; (f) health hazard—select materials that are nontoxic, nonradioactive, and so on; and (g) cost—select materials that can be manufactured at a reasonable cost.

Although these criteria have been discussed in previous publications,[17] it is worthwhile to emphasize a few points here. First, it is crucial for a high-reflectance multilayer mirror to have a good spacer. As a rule of thumb, those materials that have an absorption edge in the spectral region of interest will be good spacers at wavelengths just above the edge. Next, one must find a second material that gives the maximum optical contrast with the spacer material while still having an extinction coefficient as low as possible. The first two criteria listed above are fundamental and should always be met. In practice, these two criteria are always used simultaneously because a search is made for material pairs that have optical constants that result in a high theoretical reflectance for ideal multilayer structures. The search for high-reflectance material pairs can be done with the assistance of a computer program[18] or with graphical methods.[19] The next two criteria, (c) and (d), concern the quality of the layers and their interfaces. Ideal multilayer coatings would have smooth and continuous layers, but the morphology of real layers depends on factors that affect film growth, such as the surface adatom mobility and free surface energy. These factors are in turn related to the deposition process parameters and the properties of the

Table 1. Best Spacers for Different Wavelength Regions

Wavelength Region (nm)	Spacers	R_{max} (%)
2.8–3.6	Sc, Ti, Ba, Be, Mg	~30–40
3.6–6.7	Ca, C, Ba	~45–55
6.7–11.5	B, B_4C, Ca	~55–65
8.0–12.0	Sr, B, Y, Be	~60–80

specific materials. In addition, the chemical reactivity and miscibility of a material pair are important as they determine the likelihood of the formation of alloys or compounds that increase the interface width. This information can be gathered from binary phase diagrams, enthalpy of formation tables, and diffusion coefficient tables. Finally, the quality of the films is also related to their chemical reactivity with respect to contaminants that may be present during deposition. A UHV process may be required to deposit layers of highly reactive materials without any contamination. In addition, capping layers may be required to prevent deterioration of the multilayer in its ambient environment after deposition.

Unfortunately, it is not certain *a priori* whether or not a given criterion is satisfied for a particular material pair. This is why exploratory experiments have been performed. In addition, some of the above criteria are based on theoretical values that may not be accurate. Hence, it may be worthwhile to deposit some material pairs even if one or more criteria do not appear to be satisfied.

The selection of the best material pairs was focused mainly on elements and not on compounds. We used this approach because elemental multilayers usually have higher theoretical reflectances than multilayers made with related compounds. This is because, in the wavelength region of interest, the optical constants of alloys are approximately a weighted average of the optical constants of their constituent elements. Thus, in the absence of large density changes, alloying a second element with the best element will only make the optical constants less favorable. The only compound material we considered was B_4C, as discussed in Subsection 4.B.

However, not all the elements in the periodic table can be considered as candidate materials for the fabrication of XUV multilayer mirrors. For example, all elements with melting points below 150 °C were eliminated because XUV mirrors must withstand temperatures greater than this in many applications. Also, for obvious reasons, all elements that are highly reactive or radioactive were eliminated from further considerations.

The first step in the material pair selection process was carried out by using a procedure similar to that outlined by Rosenbluth.[18] Briefly, this method uses the optical constants of a given pair of materials to estimate quickly the maximum normal incidence peak reflectance, assuming ideal interfaces. The optical constants of the elements used in this study

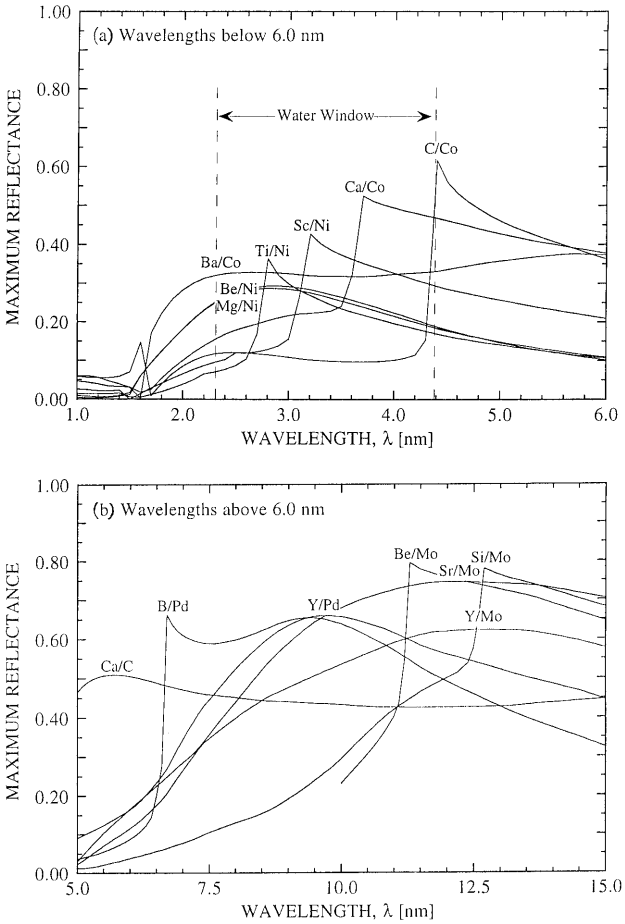

Fig. 1. Maximum achievable normal incidence peak reflectance of ideal multilayers (N = 500 bilayers) consisting of selected pairs of materials for wavelength regions of (a) 1–6 nm, (b) 5–15 nm. The optical constants of the materials used in these calculations were derived from the scattering factors of Henke *et al.*,[20] assuming bulk density for the layers.

were derived from the scattering factors of Henke *et al.*[20] by using bulk densities for the elements.

The best spacers for different wavelength regions are shown in Table 1. Figures 1(a) and 1(b) show the maximum achievable normal incidence peak reflectances of multilayers based on these spacers in the 2- to 15-nm wavelength region. The calculations were made by assuming ideal multilayers with N = 500 periods with the optimal layer thicknesses for each wavelength. For the sake of clarity, only one material pair combination is plotted for each spacer in the different wavelength ranges of interest. The choice of absorber materials in Fig. 1 is arbitrary and other combinations could yield similar reflectances. The major features of these reflectance curves coincide with absorption edges of the spacer materials. The sharpness of the falloff in reflectance associated with the associated edge depends on whether the absorption edge corresponds to electronic transitions involving core or outer atomic levels, i.e., sharper for K edges and smoother for M edges. Note that in these figures, as in the rest of this paper, the material pairs

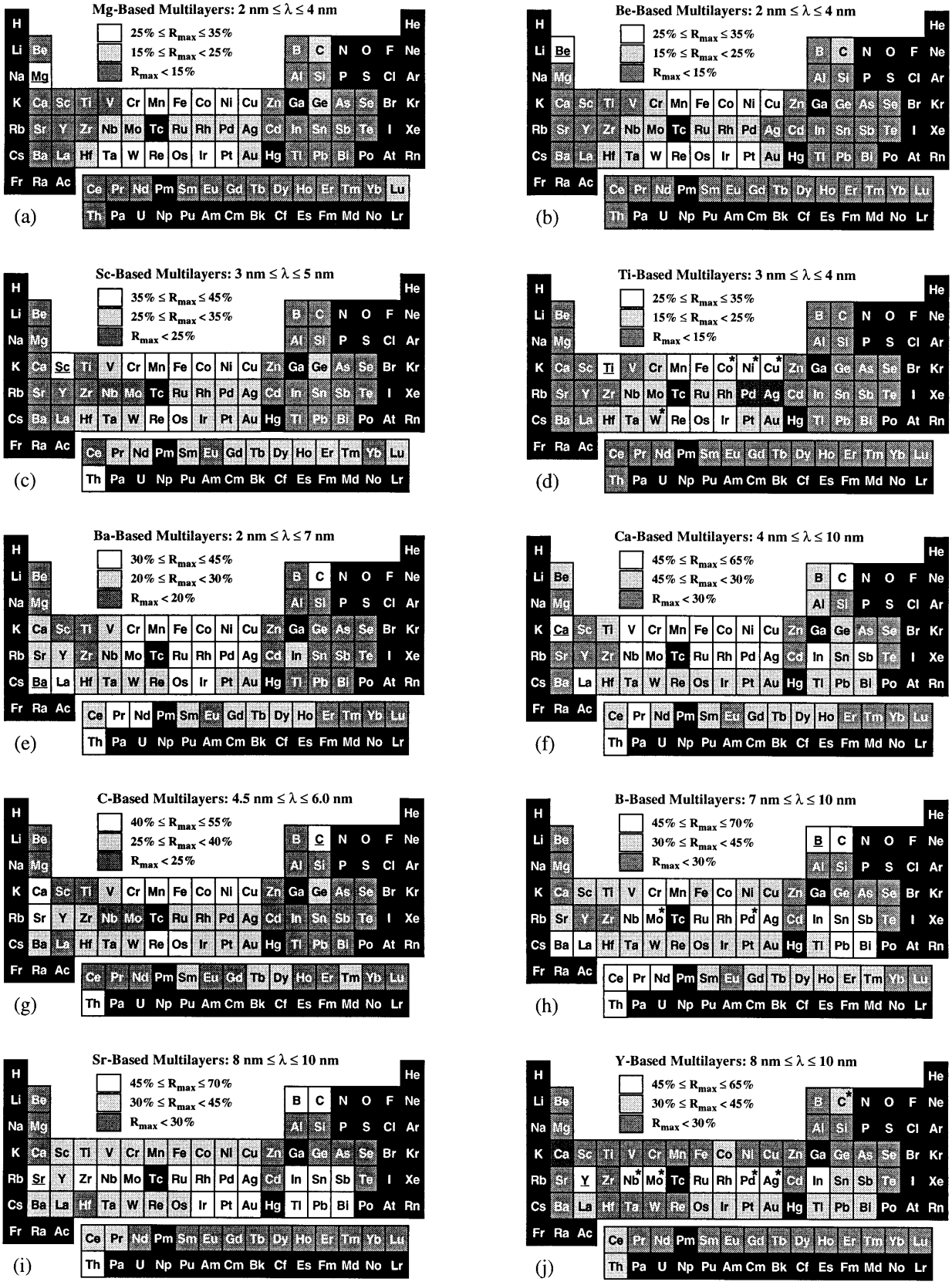

Fig. 2. Theoretical peak reflectances that can be achieved when the (a) Mg, (b) Be, (c) Sc, (d) Ti, (e) Ba, (f) Ca, (g) C, (h) B, (i) Sr, (j) Y spacers are combined with different absorbers to form multilayer mirrors for a given wavelength region. See text for details.

are denoted by using the format Xs/Xa, where Xs is the spacer and Xa is the absorber material, respectively.

Figures 2(a)–2(j) are periodic table diagrams showing the range of theoretical reflectance that the different elements can achieve when combined with the best spacers for a given wavelength region. The elements are shaded from gray to white according to the best reflectance they can achieve when combined with the spacer. The black shading was applied to elements that were not considered for the reasons stated above. Asterisks indicate the absorbers that are considered in this study.

Since the Ba, Ca, and Sr spacers are highly reactive with oxygen and water vapor, these spacer materials were not studied because special handling techniques in UHV conditions would have been required. Beryllium was not considered because of its high toxicity, Sc because of its cost, and Mg because of its high reactivity with most other materials. Finally, C was also eliminated from the selection because this spacer material has been the object of numerous previous studies. Thus, the only spacers we chose to investigate further were Ti, B, B_4C, and Y. The best absorbers for each of these spacers can be chosen from Fig. 2. Of these absorbers, some were removed from further consideration for cost reasons. A more complete description of the results of this search can be found in Ref. 21.

3. Experimental Technique

All the multilayers, with the exception of B/Mo, were deposited with a magnetically enhanced dc-triode sputtering system that has been described elsewere.[21,22] Briefly, this system contains three 5.7-cm-diameter sputtering sources with adjustable chimneys to limit the deposition region to an area directly above them. The substrates are held face down on a rotating horizontal table at a distance of 11.5 cm above the sources. Only two sources were used at any one time, and the multilayers were deposited by moving the substrate back and forth over each source. The substrate was kept stationary over the source during the deposition of each layer for the time required to deposit the desired thickness.

The multilayers were deposited on float glass substrates that could be maintained at a constant temperature of approximately 20–25 °C by using a water-cooled substrate holder. Before deposition the sputtering chamber was typically pumped to a base pressure of 5×10^{-7} Torr with a 15-cm-diameter diffusion pump and a liquid-N_2 cryogenic trap. During deposition, a controlled flow of ~47 std. cm^3/min of ultrahigh pure Ar (99.999%) was used to maintain a constant pressure of 3.0 ± 0.1 mTorr. The operating target voltages and currents for each material are listed in Table 2, along with the corresponding deposition rates determined from a low-angle x-ray diffraction analysis of double multilayer structures.[23] For some multilayers, the substrate temperature, T_s, the Ar pressure, and the target voltage and current were varied to determine what effect they had on the film microstructure. With this deposition system the deposition process control was such that thickness errors were negligible.

Table 2. Target Voltages, Currents, and Associated Deposition Rates

Material	Purity (%)	Target		Deposition Rate (nm/s)
		Voltage (V)	Current (A)	
Ag	99.999	−100	0.40	0.21
B_4C	99.9	−300	1.00	0.04
Co	99.91	−150	0.50	0.08
Cu	99.999	−150	0.50	0.24
Mo	99.95	−175	1.00	0.29
Nb	99.91	−175	0.60	0.10
Ni	99.991	−150	0.50	0.09
Pd[a]	99.99	−100	0.75	0.22
Pd	99.99	−175	0.40	0.36
Ti	99.91	−150	0.50	0.05
W	99.95	−150	0.50	0.07
Y[b]	99.9	−175	1.00	0.43
Y	99.9	−175	0.40	0.21

[a]When Pd is deposited with B_4C (the next Pd row corresponds to Y).
[b]When Y is deposited with Mo (the next Y row corresponds to Ag, Nb, Pd, and C).

After deposition, each multilayer was immediately characterized by low-angle x-ray diffraction (LAXRD) by using Cu K_α ($\lambda = 0.154$ nm) radiation in a θ–2θ geometry. The LAXRD spectrum of a typical multilayer mirror consists of a series of Bragg peaks from which the multilayer period, Λ, and the relative absorber layer thickness, $\Gamma = d_a/\Lambda$, can be determined.[24] In addition, these spectra provide a basis for comparing the structure quality of different multilayers. For example, multilayers with nearly ideal structures will have a series of sharp and intense peaks up to an angle of $2\theta \cong 10°$, whereas those with rough or wide interfaces will only have peaks present at the smaller angles of this range. Spectra from the better multilayers can be fitted to yield interface width parameters, $\sigma_{\text{A-on-B}}/\sigma_{\text{B-on-A}}$. These can then be used for quantitative comparisons of the A-on-B and B-on-A interfaces, respectively. Note that the interface width parameter σ is related to the physical width of the interface, w, by the expression $\sigma = w/2\sqrt{3}$ for an error-function interface profile.[25] The scattering factors tabulated by Cromer and Liberman[26] were used for the LAXRD calculations at $\lambda = 0.154$ nm.

In some deposition runs, electronic grade Si⟨100⟩ and C (pyrolitic graphite) substrates were also simultaneously coated. The Si substrates were used for transmission electron microscopy (TEM) and depth-profile Auger electron spectroscopy (AES) analysis, whereas the C substrates were used for Rutherford backscattering spectroscopy (RBS) analysis. For the TEM analysis, ultrathin cross-sectional specimens were prepared by a two-step process involving mechanical polishing and ion-beam milling.[27] High-resolution images were obtained by using a JEOL 2000FX TEM instrument operated at 200 kV with a point-to-point resolution of ~0.4 nm.

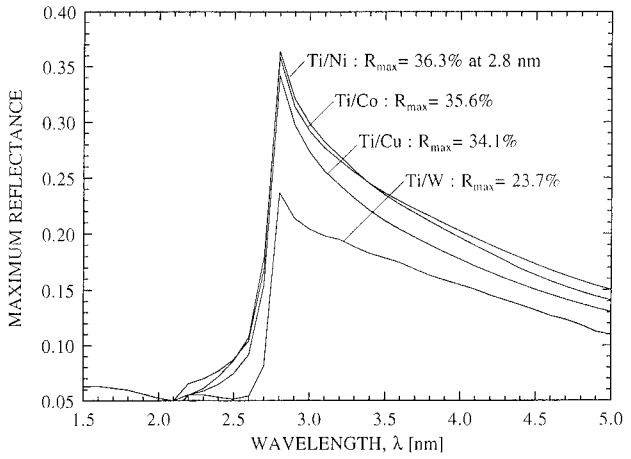

Fig. 3. Maximum achievable normal incidence peak reflectance for ideal Ti/Ni, Ti/Co, Ti/Cu, and Ti/W multilayers consisting of $N = 500$ bilayers.

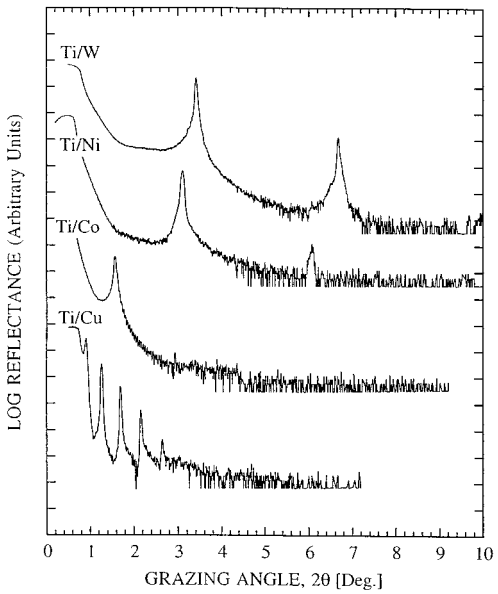

Fig. 4. Typical LAXRD spectra for the Ti/W, Ti/Ni, Ti/Co, and Ti/Cu multilayers deposited in this study.

The most promising multilayer mirrors for each material pair, as judged by their LAXRD spectra, were characterized by measuring their near-normal incidence reflectance versus wavelength in the XUV spectral regions of interest. These measurements were performed at the Canadian Synchrotron Radiation Facility (CSRF) at the University of Wisconsin-Madison by following a procedure described previously.[23] This reflectometer uses a grasshopper-type monochromator that has a spectral range extending from 1.0 nm to 20.0 nm (60 to 1500 eV) with a resolution of 0.03 nm. The absolute reflectance was measured to an accuracy of $\pm 1\%$ by measuring both the incident and reflected beams and then by taking a ratio of these two measurements after they were compensated for the decay of the synchrotron beam current. It should be noted that these normal incidence reflectance measurements were performed at the end of the study and were not used to optimize the deposition conditions.

4. Experimental Results

We have investigated Ti-, B- or B_4C-, and Y-based multilayers for the 2.8- to 3.6-nm, 6.7- to 11.5-nm, and 8.0- to 12.0-nm wavelength ranges, respectively.

A. Ti-Based Multilayer Mirrors for the 2.8- to 3.6-nm Wavelength Region

According to the theoretical search described in Section 2, Ni, Co, Cu, or W absorbers used in conjunction with a Ti spacer can achieve high reflectances in the water window wavelength region. The maximum achievable peak reflectance curves for these four material pairs are shown in Fig. 3. Maximum normal incidence peak reflectances near 35% at $\lambda \cong 2.8$ nm are predicted when Ti is paired with Ni, Co, and Cu, whereas a lower maximum of ~24% is predicted for the Ti/W pair. Note, however, that at least 350 periods with layer thicknesses of the order of 0.6–0.8 nm are required to achieve these reflectances.

To our knowledge, Ti/Co and Ti/Cu have never been considered as material pair candidates for XUV multilayer mirrors. However, the magnetic properties of Ti/Co multilayers as well as the microstructural and diffusion properties of both pairs have been investigated by others.[28–32] There have been some early studies on the annealing behavior of Ti/W multilayers,[33] but its use in XUV multilayer mirrors is fairly recent.[34] There has been a large body of reported research on the magnetic,[35] neutron reflectivity,[36,37] and diffusion[38–43] properties of Ti/Ni multilayers. Although a few Ti/Ni multilayer mirrors have been previously fabricated for the XUV wavelength region between 2.7 and 4.1 nm, they were not designed for normal incidence.[44–46]

The LAXRD spectra for the above Ti-based pairs are shown in Fig. 4. The spectrum for the Ti/W multilayer appears to be qualitatively the best, having a large Bragg peak past $2\theta = 6°$. Simulations of the LAXRD spectra, assuming an error-function interface profile,[14] indicated that interface widths of $\sigma \sim 1.5$–2.0 nm were present in all the multilayers except for the Ti/W multilayer, which had $\sigma \sim 0.3$–0.7 nm. Note that the large interface widths in the Ti/Co and Ti/Cu multilayers may have been a result of their relatively thick layers. Further investigations of these material pairs, in particular Ti/Cu, are needed to be able to judge ultimate performance.

Because the Ti/W multilayer was the best of this series, we studied this material pair in more detail. The measured LAXRD spectrum for a Ti/W multilayer with 100 periods of 2.66-nm thickness is shown in Fig. 5. Also shown is a theoretical fit to the measured data. The interface widths used in the fit are $\sigma_{\text{Ti-on-W}} = 0.41$ nm and $\sigma_{\text{W-on-Ti}} = 0.62$ nm ($\sigma = 0.41/0.62$ nm). The normal incidence peak reflectance calculated with these interface width parameters is

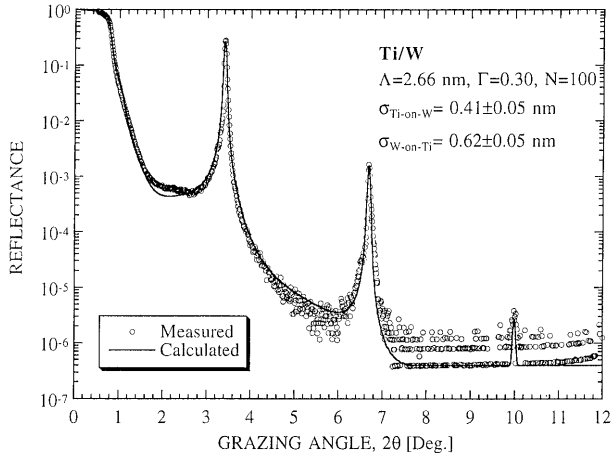

Fig. 5. LAXRD measurement of a typical Ti/W multilayer accompanied by the best theoretical fit to the measured data. The parameters used for the fit are shown. A divergence $\Delta 2\theta = 0.02°$ of the incident x-ray beam as well as a constant background $R_{bkgd} = 4 \times 10^{-7}$ have been included in the fit model.

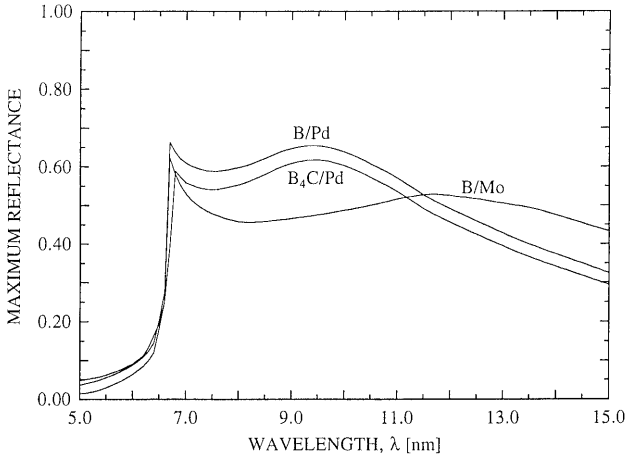

Fig. 6. Maximum achievable normal incidence peak reflectance for ideal B/Pd, B_4C/Pd, and B/Mo multilayers consisting of $N = 500$ bilayers. The B/Pd material pair was not investigated in this study but its curve is shown for comparison.

only 0.3% at $\lambda = 2.8$ nm. This reflectance is much lower than the 15% value calculated for an ideal 100-period mirror at normal incidence. Although the interface width in this Ti/W multilayer compares favorably to that of most other multilayers, the reflectance is strongly reduced because the interface is a large fraction of the Ti and W layer thicknesses. We also observed, from both LAXRD and TEM measurements made on additional samples, that the interface roughness increased markedly as the number of periods was increased.

To avoid the high interface width-to-layer thickness ratio obtained with the previous design, we fabricated additional multilayers that were designed for maximum reflectance at an oblique angle of incidence, $\alpha = 60°$, and $\lambda = 2.8$ nm. Assuming the interface widths were the same as those determined above and that the incident light was 90% *s* polarized, we calculated a peak reflectance of 7.1% for a 100-period mirror. To study the dependence of the reflectance on the number of layers with this design, we also made a multilayer mirror with only 60 periods. For the 100-period mirror we measured a peak reflectance of $4.1 \pm 0.1\%$ at $\lambda = 2.80$ nm and $\alpha = 59°$. For the 60-period mirror we measured a slightly higher peak reflectance of $5.2 \pm 0.1\%$ at $\lambda = 2.79$ nm and $\alpha = 61°$. Hence, it appears that under these deposition conditions the optimum number of periods for the Ti/W system is near 60.

Another 60-period Ti/W multilayer was fabricated without substrate cooling to see if the higher substrate temperature would influence the interface roughness. With cooling the substrate temperature was constant at ~25 °C, whereas without it the substrate temperature rose throughout the deposition run, reaching a maximum temperature of $T_s \sim 85$ °C. The LAXRD measurements on this sample showed that the interface quality was worse than that obtained with substrate cooling. Not surprisingly, this sample had a lower measured peak reflectance of $3.0 \pm 0.2\%$ at $\lambda = 2.79$ nm and $\alpha = 61°$, which is nearly half of that of its cooled counterpart.

B. B- and B_4C-Based Multilayer Mirrors for the 6.7- to 11.5-nm Wavelength Region

As shown in Section 2, both B and B_4C are promising spacer materials in the 6.7- to 11.5-nm wavelength region. Although B is theoretically a better spacer than B_4C, the latter was studied first because it is much easier to deposit by sputtering. From the predicted performances and the availability of the sputtering targets, Pd and Mo were selected as absorber materials to form B_4C/Pd and B/Mo multilayers. Figure 6 shows the maximum achievable peak reflectances that can be obtained with ideal B_4C/Pd and B/Mo multilayer mirrors in the 5- to 15-nm range. It should be noted that although similar material pairs such as B/Pd, B_4C/Mo, and (B + C)/Mo have been investigated by others,[47–51] to our knowledge the B_4C/Pd and B/Mo material pairs have not been previously examined.

We designed and fabricated several B_4C/Pd multilayer mirrors for maximum normal incidence reflectance at $\lambda = 8.5$–9.0 nm with $\Lambda = 4.4$ nm, $\Gamma = 0.40$ and $N = 50$. The LAXRD spectra for these multilayers showed that they had a good layer quality with interface widths in the range $\sigma \sim 0.4$–0.6 nm. As with Ti/W, we made similar samples with and without substrate cooling. Without substrate cooling, the final substrate temperature at the end of the deposition run was $T_s = 90$ °C. As shown in Fig. 7, the near-normal incidence peak reflectance of the cooled and uncooled samples are $11.5 \pm 0.2\%$ at $\lambda = 8.46$ nm and $6.2 \pm 0.1\%$ at $\lambda = 8.89$ nm, respectively. The lower reflectance for the uncooled sample is consistent with an increase in interface width σ from 0.35/0.55 nm to 0.50/0.85 nm, as determined from an analysis of the LAXRD spectra.

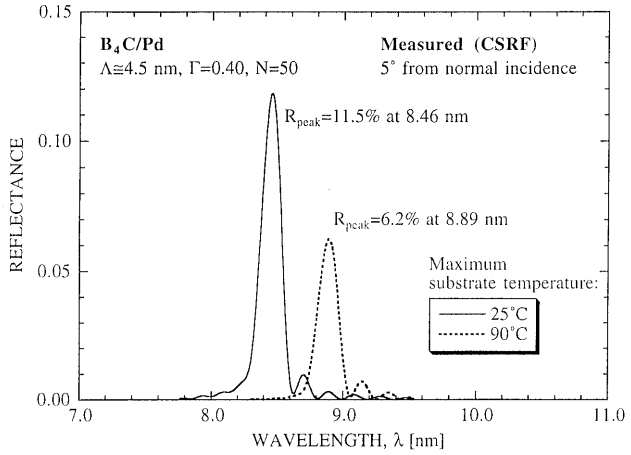

Fig. 7. Measured XUV reflectance of two B_4C/Pd multilayers deposited at different substrate temperatures.

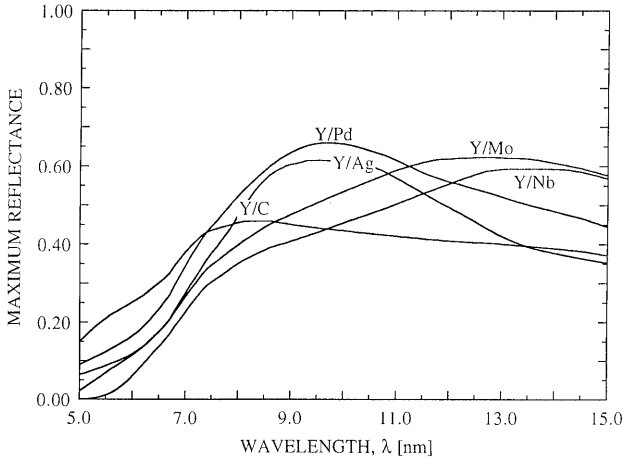

Fig. 9. Maximum achievable normal incidence peak reflectance for ideal Y/Pd, Y/Ag, Y/Mo, Y/Nb, and Y/C multilayers consisting of $N = 500$ bilayers.

The B/Mo multilayers were made by using a different deposition system that had a cryopumped vacuum chamber with two 5.1-cm-diameter magnetron sputtering guns.[52] The Mo target was dc sputtered, whereas the B target was rf sputtered because of its low conductivity. The B target was 99.9% pure and had a density of only ~ 1.04 g/cm^3, which is 45% of the bulk value. Constant powers of 100 W (dc) and 200 W (rf) were applied to the Mo and B targets, respectively, and the sputtering pressure was maintained at 2.0 ± 0.1 mTorr. With these operating conditions the deposition rates for the Mo and B layers were 0.09 nm/s and 0.01 nm/s, respectively. Figure 8 shows the reflectance curve for a B/Mo multilayer deposited on a Si substrate with $\Lambda = 3.35$ nm and $N = 100$ periods. This mirror had a measured peak reflectance of $9.4 \pm 0.2\%$ at $\lambda = 6.67$ nm and $\alpha = 5°$. According to the LAXRD spectra, the overall structure of this B/Mo multilayer is good, with interface widths of $\sigma \cong 0.35/0.65$ nm.

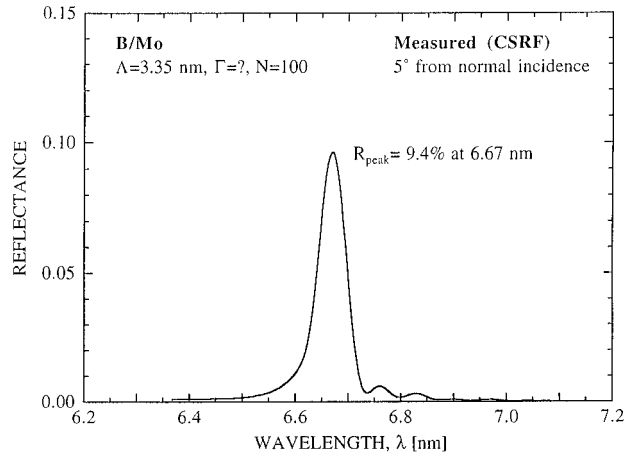

Fig. 8. Measured XUV reflectance of a B/Mo multilayer.

C. Y-Based Multilayer Mirrors for the 8.0- to 12.0-nm Wavelength Region

According to the search described in Section 2, Y is an excellent spacer material for the 8.0- to 12.0-nm wavelength region. When Y is combined with absorbers such as Pd, Rh, Ru, Ag, Mo, Nb, In, and C, calculations show that normal incidence reflectances between 45% and 65% can be achieved for ideal multilayers. We made multilayers with all the absorbers listed above except for Rh, Ru, and In. The theoretical reflectance curves of these Y-based multilayers are shown in Fig. 9. To our knowledge, except for publications that arose from this research,[52,53] there has been no previous research on Y as a spacer material for XUV multilayer mirrors.

Figure 10 shows typical LAXRD spectra for each

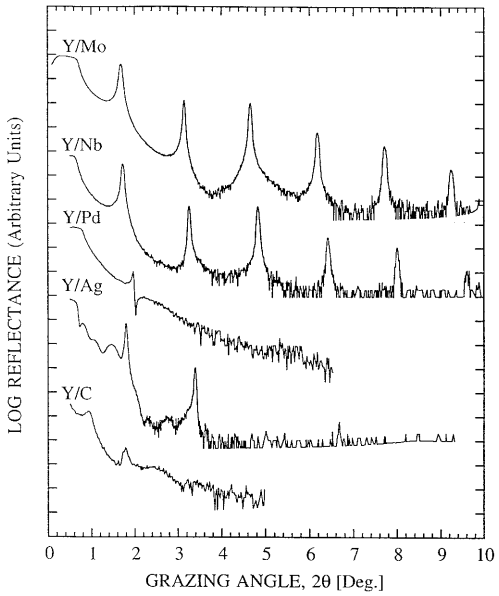

Fig. 10. Typical LAXRD spectra for the Y/Pd, Y/Ag, Y/Mo, Y/Nb, and Y/C multilayers deposited in this study.

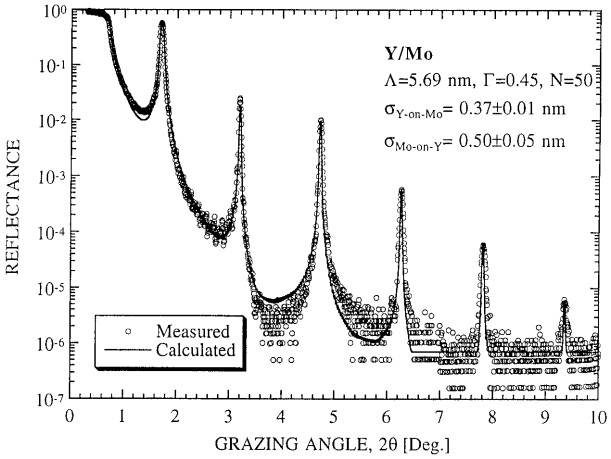

Fig. 11. LAXRD measurement of a typical Y/Mo multilayer accompanied by the best theoretical fit to the measured data. The parameters used for the calculation are shown in the figure. A divergence $\Delta 2\theta = 0.02°$ of the incident x-ray beam as well as a constant background $R_{bkgd} = 4 \times 10^{-7}$ have been included in the fit.

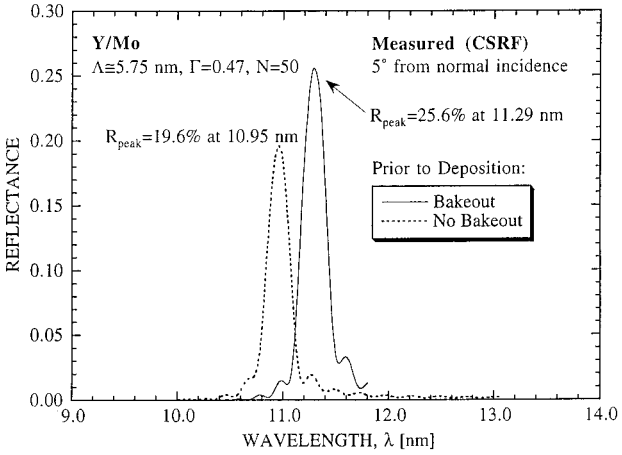

Fig. 12. Measured XUV reflectance of two Y/Mo multilayers deposited with and without chamber bakeout prior to deposition.

material pair. It is evident from these spectra that both the Y/Ag and Y/C material pairs formed multilayers with significant interface roughness, intermixing, or both. In successive LAXRD scans made over a 48-h period, the original Bragg peaks gradually broadened and diminished, indicating that both types of multilayers were unstable. In the case of Y/C, the Bragg peaks vanished altogether and the multilayer became transparent. Apparently, a new compound formed during that period. In the case of Y/Ag, a RBS analysis of the multilayers made after a few days of exposure to air showed that they contained ~50 at. % oxygen. Fits of the LAXRD spectra of the Y/Pd multilayers were consistent with the formation of thick Pd-rich compound layers that left only ~0.2 nm of pure Y out of the ~2.6 nm deposited originally for each Y layer. A high-angle x-ray diffraction analysis of a Y/Pd multilayer suggested that the compound formed was YPd_3. The measured normal incidence XUV reflectances at a wavelength of ~11 nm for these material pairs were $R_{Y/Pd} < 0.5\%$, $R_{Y/Ag} < 0.2\%$, and $R_{Y/C} \cong 0\%$. Hence, it follows from Fig. 10 that only the Y/Mo and Y/Nb combinations resulted in good-quality multilayers. Because Y/Mo had a higher predicted reflectance than Y/Nb (Fig. 9), we selected the Y/Mo pair for further study.

Figure 11 shows the LAXRD spectrum of a 50-period Y/Mo multilayer designed for maximum normal incidence reflectance at $\lambda = 11.0$ nm. The theoretical fit, shown as a solid curve in the figure, yielded the following structural parameters: $\Lambda = 5.69$ nm, $\Gamma = 0.45$, $\sigma = 0.37/0.50$ nm. From these parameters we calculated a normal incidence peak reflectance of 44.1% at $\lambda = 11.0$ nm, but the measured peak reflectance was only $19.6 \pm 0.1\%$ at 5° from normal incidence.

A RBS analysis indicated that the Y/Mo multilayers contained approximately 7 at. % oxygen. This oxygen contamination was also verified by AES sputter depth profiling. In addition, the depth profiles showed that the oxygen contents were higher at the multilayer surface and decreased within a few periods to a nonzero level, primarily concentrated in the Y layers. From these results, it appears that oxidation of the Y layers, either during deposition or after exposure to air, is a significant factor in causing the lower than expected reflectance. To determine if the contamination occurred during the deposition, we deposited a second Y/Mo multilayer under nominally the same conditions as the previous multilayer except that a chamber bakeout preceded the deposition. This second multilayer had a peak reflectance of $25.6 \pm 0.2\%$ as shown in Fig. 12. Because the LAXRD spectra indicated that both of these multilayers had the same high-quality multilayer structure, a change in the interface imperfection can be ruled out as a possible explanation for the difference. This supports the argument that the improvement in the reflectance is a result of minimizing residual gas contamination during deposition.

In an attempt to improve the performance of the Y/Mo multilayers further, different deposition conditions were investigated, including higher target voltages, no substrate cooling, and higher sputtering pressures. Among these deposition parameter variations, only the sputtering pressure had a significant effect on the quality of the multilayers. A multilayer deposited at the higher pressure of 6 mTorr had a peak reflectance of only $12.1 \pm 0.1\%$ at $\lambda = 11.6$ nm. Furthermore, from an analysis of the LAXRD curves, we found that interface width σ increased from 0.37/0.50 nm to 0.65/0.75 nm as the pressure was increased from 3 to 6 mTorr.

5. Analysis and Discussion

Table 3 summarizes the results for the best multilayer samples made with each material pair. The structure of each sample is described by parameters N, Λ, Γ, and σ, as determined by LAXRD analysis. The measured peak reflectance and, more impor-

Table 3. Characterization Results of the Best Multilayer Samples for Each Material Pair

Material Pair (A/B)	N	Λ (±0.01) (nm)	Γ (±0.02)	σ (±0.1) (nm)	α (deg)	λ_{peak} (nm)	Peak Reflectance (%) R_m	Peak Reflectance (%) R_t	$\beta = R_m/R_t$
Ti/Co	10	9.25	0.47	1.1/1.6	—	—	—	—	—
Ti/Ni	100	2.92	0.40	1.5/1.8	62	2.79	0.2 ± 0.1	39.1 ± 0.1	≤0.01
Ti/Cu	30	17.42	0.84	2.0/3.0	—	—	—	—	—
Ti/W	60	2.82	0.29	0.4/0.7	61	2.79	5.2 ± 0.1	24.3 ± 0.1	0.21 ± 0.01
B_4C/Pd	50	4.36	0.40	0.4/0.6	5	8.46	11.5 ± 0.2	38.4 ± 1.6	0.30 ± 0.02
B/Mo	100	3.35		0.4/0.7	5	6.67	9.4 ± 0.2	—	—
Y/Pd	60	4.95		1.0/1.5	5	9.69	0.3 ± 0.1	63.2 ± 1.0[a]	≤0.01
Y/Ag	70	5.33	0.43	1.0/1.8	5	10.80	0.1 ± 0.1	57.8 ± 1.0	≤0.01
Y/Mo	50	5.75	0.47	0.3/0.6	5	11.29	25.6 ± 0.2	51.9 ± 0.4	0.49 ± 0.01
Y/Nb	50	5.54	0.46	0.3/0.6	5	10.94	9.4 ± 0.1	37.5 ± 0.4	0.25 ± 0.01
Y/C	30	4.10		>1.0	—	—	—	—	—

[a]A value of $\Gamma = 0.46$ was assumed for this calculation.

tantly, the reflectance ratio $\beta = R_m/R_t$, i.e., the ratio of the measured to the theoretical (ideal) peak reflectance, for each multilayer is also listed in this table. Reflectance ratio β is useful for comparing the performance of different mirrors at different wavelengths or angles of incidence. One must keep in mind, however, that high β values are more difficult to obtain for smaller Λ because the width of the interface imperfections tends to be a larger fraction of the layer thickness. When calculating the theoretical peak reflectance, we used the experimentally determined Λ and Γ values, assumed no interface imperfections or layer contamination, and used the same wavelength and angle of incidence as the measured peak reflectance. For some material pairs we did not calculate a value for β because either XUV reflectance R_m was not measured or because we were not able to determine the structural parameters with sufficient accuracy.

The multilayer mirrors fabricated in this study were based on material pairs that were selected primarily because of their optical properties. However, as we can see from the above results, the measured reflectances were generally much lower than predicted, i.e., the β values were between 0.0 and 0.5. Since thickness errors were negligible, the ultimate performance of each multilayer was limited by interface imperfections or (and) layer impurities. Interface imperfections include roughness and intermixing. Roughness at the interfaces can result from the microstructure of the layers, whereas intermixing between material pairs is due to interdiffusion or compound formation. Impurities or contaminants can be incorporated into the layers either during deposition or after the sample is exposed to ambient air.

An important part of interpreting these results is distinguishing between effects that are intrinsic (or fundamental) to a given material pair and effects that are a result of the deposition process or the environment. This distinction is necessary if we are to determine if a significant improvement can be achieved with a particular material pair. For example, one has little control over intermixing at the interfaces because this depends primarily on the materials themselves. There is some control, however, over the interface roughness and chemical purity because they are partially dependent on the deposition process. Therefore, if the performance is limited by wide interfaces formed through intermixing, then it may not be possible to reduce the interface width below a fundamental thickness. However, if the performance of a multilayer pair is limited primarily by layer roughness or poor film quality, then it may be possible to improve the multilayer.

First, let us consider the processes that are difficult to control, i.e., compound formation and interdiffusion at the interfaces. The probability of forming a compound from two materials is given by the Gibbs free energy of formation, defined as $\Delta G^\circ = \Delta H^\circ - T\Delta S^\circ$, where ΔH° and ΔS° are the enthalpy and entropy of formation, respectively. Physically, ΔG° corresponds to the amount of energy required to form a compound from its constituent elements. With a large negative ΔG° value, a compound is more likely to form because energy is being released during the reaction. A problem with using ΔG° in practice is that entropy of formation ΔS° is difficult to measure experimentally. However, for solid–solid interactions such as those occurring at the interfaces of the multilayers investigated in this study, ΔS° is small so that $\Delta G^\circ \cong \Delta H^\circ$. Note that ΔG° (or ΔH°) does not indicate whether or not interdiffusion will occur between materials. For each material pair A/B investigated, Table 4 lists the overall quality of the deposited multilayers along with the calculated ΔH°_{calc} (AB) value for compound AB.[54] Also listed in the table are the calculated and experimentally determined $\Delta H^\circ(A_xB_y)$ values for the compound A_xB_y that is most likely to form.[54] Note that ΔH°_{calc} (AB), given for each material pair A/B, is used for comparison purposes and that some of these AB compounds may not actually exist.

From Tables 3 and 4, one can see that the best results were obtained with the material pairs that have positive or only slightly negative ΔH° values and that do not form compounds according to binary phase diagrams. This is the case for Ti/W, B_4C/Pd, Y/Nb, and Y/Mo, which had reflectance ratios β of

Table 4. Enthalpy of Formation of Some Compounds for Each Material Pair[a]

Parameter	Ti-Based Pairs				B-Based Pairs		Y-Based Pairs				
	Ti/Co	Ti/Ni	Ti/Cu	Ti/W	B_4C/Pd	B/Mo	Y/Pd	Y/Ag	Y/Mo	Y/Nb	Y/C
Multilayer quality	Poor	Poor	Poor	Good	Good	Good	Poor	Poor	Good	Good	Poor
ΔH°_{calc} (AB) (kJ/mol)	−42	−52	−13	−9	—	−49	−123	−44	+35	+44	−72
Compound (A_xB_y)	TiCo	$TiNi_3$	$TiCu_4$	None	B_2Pd_5	BMo	YPd_3	YAg	None	None	Y_2C_3
ΔH°_{exp} (A_xB_y) (kJ/mol)	−44	−35	−23	—	+45	−62	−94	−26	—	—	−51
ΔH°_{calc} (A_xB_y) (kJ/mol)	−42	−37	−7	—	—	−49	−90	−44	—	—	−78

[a]Values given for T = 298 K except for the ΔH°_{exp} of YPd_3 (T = 1023 K), YAg (T = 1346 K) and Y_2C_3 (T = 1700 K).

0.21, 0.30, 0.25, and 0.49, respectively. The Ti/Cu multilayer was of poor quality even though this material pair has a small negative ΔH° value, but this may have been a result of layer roughness caused by its unusually thick layers. All the other material pairs, i.e., Ti/Co, Ti/Ni, B/Mo, Y/Pd, Y/C, and Y/Ag, had large negative ΔH° values. With the exception of B/Mo, which formed a good-quality multilayer, the remaining multilayer mirrors were of poor quality and had low reflectance ratios β.

From the above results there appears to be a strong correlation between the multilayer quality and the ΔH° value. A similar correlation between ΔH° and the multilayer quality has been discussed by others in the field of XUV multilayer mirrors.[50] In general, material pairs with a large positive ΔH° value have the potential to form good-quality multilayers. However, the quality of these multilayers may be limited by other mechanisms such as interdiffusion, interface roughness, or layer contamination. Material pairs with a large negative ΔH° value are unlikely to form good multilayer mirrors because they have a tendency to form compounds that tends to broaden the interfaces. The quality of these multilayers, however, will depend on the final width of the compound layer, which in turn depends on whether or not the compound layer is a good diffusion barrier with respect to its constituent elements. For example, the Y/Pd multilayers were of poor quality because relatively large interfaces of YPd_3 were formed. In contrast, it is known[24] that the Si/Mo material pair forms good multilayers even though $MoSi_2$ compound layers are forming at the interfaces [$\Delta H^\circ(MoSi_2)$ = −44 kJ/mol (Ref. 54)]. The reason for the good multilayers is that the compound layer remains thin, i.e., it is in effect a good self-limiting interdiffusion barrier that prevents it from getting any thicker. Similarly, a thin stable interdiffusion barrier may explain why the B/Mo multilayer was of good quality even though it had a large negative ΔH° value. Another possible explanation might be that impurities in the B target formed compounds in the B layer that would not react or interdiffuse with Mo.

Next, let us consider the processes that we may be able to control, i.e., interface roughness and layer contamination. The quality of the multilayers based on material pairs that had positive or slightly negative ΔH° values, such as Ti/W, B_4C/Pd, and Y/Mo, was not as good as expected. The interface roughness of XUV multilayer mirrors is dependent on deposition parameters such as substrate temperature, sputtering gas pressure, substrate-to-target distance, and so on. Varying the substrate temperature affected the interface roughness of both the Ti/W and the B_4C/Pd multilayers. The increase in interface roughness with substrate temperature may be the result of the higher adatom mobility that resulted in a coalescence of larger clusters or islands, i.e., a more three-dimensional growth mode. Increasing the sputtering gas pressure in the deposition of the Y/Mo multilayers also resulted in an increased interface roughness. This effect is well known and has been seen most notably in Si/Mo XUV multilayers mirrors.[24,55,56] Essentially, there is an enhanced columnar growth as the sputtering gas pressure is increased because of atomic shadowing acting in concert with low adatom mobilities.[55,57] However, the change of the above deposition parameters in this study only led to an increase in interface roughness and, hence, to a lower reflectance ratio β.

Table 5. Free Energy of Formation of the Most Probable Solid Oxide, Nitride, and Carbide for Each Element[a]

Compound	Ti	Co	Ni	Cu	W	B	Y	Pd	Ag	Mo	Nb	C
Oxide (A_xO_y)	Ti_2O_3	Co_3O_4	NiO	Cu_2O	WO_3	B_2O_3	Y_2O_3	PdO	Ag_2O	MoO_3	Nb_2O_5	—
ΔG°_{exp} (A_xO_y) (kJ/mol)	−1434	−787	−213	−145	−764	−1193	−1817	−82	−11	−668	−1766	—
Nitride (A_xN_y)	TiN	Co_3N	Ni_3N	CuN_3	—	BN	YN	—	AgN_3	Mo_2N	Nb_2N	CN
ΔG°_{exp} (A_xN_y) (kJ/mol)	−308	+34	+7	+67	—	−226	−269	—	+376	−50	−218	+427
Carbide (A_xC_y)	TiC	Co_2C	Ni_3C	—	WC	B_4C	YC_2	—	—	Mo_2C	Nb_2C	—
ΔG°_{exp} (A_xC_y) (kJ/mol)	−180	+14	+32	—	−39	−72	−109	—	—	−47	−182	—

[a]Values given for T = 298 K.

Concerning layer contamination, Table 5 lists the oxide, nitride, and carbide compounds most likely to form as a result of contamination during deposition or after exposure to air for each element investigated in this study. The experimentally determined $\Delta G°_{exp}(A_xO_y)$, $\Delta G°_{exp}(A_xN_y)$, and $\Delta G°_{exp}(A_xC_y)$ are given for the oxides, nitrides, and carbides, respectively.[58,59] When considering the formation of oxides or nitrides, it is necessary to use $\Delta G°$ rather than $\Delta H°$ because entropy of formation $\Delta S°$ can be significant in such gas-solid reactions.

The values of Table 5 show that Y, Ti, Nb, and B are the most reactive elements, especially with oxygen. Therefore, when these materials are used, there is a strong possibility of oxygen contamination both during deposition and when the sample is exposed to the atmosphere. Our observation that a chamber bakeout before the deposition of an Y/Mo multilayer resulted in a higher reflectance ratio could be the result of reduced oxygen contamination, because the amount of water vapor in the sputtering environment has been decreased. Similarly, the lower reflectance ratio β for the Y/Nb multilayer compared with that of the Y/Mo multilayer, even though the two types of multilayers had a similar high-quality structure according to the LAXRD measurements, might be a result of the higher $\Delta G°$ for Nb_2O_5 compared with that for MoO_3.

More research on Y/Mo multilayers has been performed since this preliminary survey was undertaken.[52,53] These subsequent studies have shown that both layer contamination during deposition and surface oxidation after deposition were responsible for the lower than expected reflectances seen in this study. A 100-period Y/Mo multilayer made in a UHV deposition system had a near-normal incidence peak reflectance of 45.8% at 11.2 nm before exposure to ambient air. After exposure to air, the peak reflectance of this multilayer decreased to 41.5% within several days and then stabilized.

The extinction coefficient of oxygen decreases quickly with decreasing wavelengths and becomes negligible in the water window wavelength region. Therefore, oxygen contamination of the Ti-based multilayer mirrors, designed to operate in the water window wavelength region, is not as severe a problem as it is for the B- and Y-based multilayer mirrors, which are designed for longer wavelengths. However, contamination by carbon and nitrogen is a problem for the Ti-based multilayer mirrors in this water window wavelength region.

6. Conclusions

The best results at near-normal incidence were achieved with Y/Mo, B_4C/Pd, and B/Mo material pairs with peak reflectances of 25.5% at 11.0 nm, 11.5% at 8.5 nm, and 9.4% at 6.7 nm, respectively. Also, at 61° from normal incidence, a peak reflectance of 5.2% at 2.8 nm was obtained with a Ti/W multilayer. For both the Ti- and Y-based multilayer series, the best reflectance results were achieved with the material pairs that had positive (or only slightly negative) enthalpies of formation $\Delta H°$ and, hence, did not form compounds according to their binary phase diagrams. These results suggest that interfacial mixing plays the dominant role in determining which material pairs can form good mirrors and that the enthalpy of formation is a valuable guide in predicting the quality that can be expected from a material pair. It appears, therefore, that it would be difficult to make significant improvements in the performance of the Ti/Co, Ti/Ni, Y/Pd, Y/C, and Y/Ag multilayer mirrors because of their negative $\Delta H°$ values. One possible way to improve the performance of these material pairs is to deposit at each interface an intermediate layer of a third material that acts as a good diffusion barrier and does not react with the original materials.[60]

It should be noted that many material pairs with high potential were not examined in this study. For example, Sr and Ca are good candidates for spacer materials if techniques can be found to prevent their exposure to air. It is likely that multilayers that use these two materials would have to be made under UHV conditions and be protected from oxidation after their deposition. In addition, some of the material pairs that were initially examined but were not investigated further might make good multilayers if deposited under different conditions. For example, the Ti/Cu material pair might make good multilayers with smaller period thicknesses.

The authors thank Y. Huai and K. Tan for their assistance in the XUV reflectance measurements at the Canadian Synchrotron Radiation Facility, J. A. Leavitt and L. McIntyre for the RBS analysis, and C. Gishey for TEM sample preparation. The research at the University of Arizona was supported by the U.S. Air Force Office of Scientific Research under contract F-49620-93-1-0201. C. Montcalm acknowledges the support of both the University of Arizona's Laboratory for X-Ray Optics and the Fonds pour la Formation de Chercheurs et Aide à la Recherche. A summary of this paper was presented in March 1994.[61]

References

1. E. Spiller, *Soft X-Ray Optics* (SPIE Optical Engineering Press, Bellingham, Wash., 1994).
2. N. M. Ceglio, "Revolution in x-ray optics," J. X-Ray Sci. Technol. **1**, 7–78 (1989).
3. D. G. Stearns, R. S. Rosen, and S. P. Vernon, "Multilayer mirror technology for soft-x-ray projection lithography," Appl. Opt. **32**, 6952–6960 (1993).
4. G. Gutman, "High-performance Mo/Si and W/B_4C multilayer mirrors for soft x-ray imaging optics," J. X-Ray. Sci. Technol. **4**, 142–150 (1994).
5. K. M. Skulina, C. S. Alford, R. M. Bionta, D. M. Makowiecki, E. M. Gullikson, R. Soufli, J. B. Kortright, and J. H. Underwood, "Molybdenum/beryllium multilayer mirrors for normal incidence in the extreme ultraviolet," Appl. Opt. **34**, 3727–3730 (1995).
6. D. G. Stearns, R. S. Rosen, and S. P. Vernon, "Normal-incidence x-ray mirror for 7 nm," Opt. Lett. **16**, 1283–1285 (1991).
7. A. D. Akhsakhalyan, N. N. Kolachevsky, M. M. Mitropolsky, E. N. Ragozin, N. N. Salashchenko, and V. A. Slemzin, "Fab-

rication and investigation of imaging normal-incidence multilayer mirrors with a narrow-band reflection in the range $\lambda \cong 4.5$ nm," Phys. Scr. **48**, 516–520 (1993).
8. I. V. Kozhevnikov, A. I. Fedorenko, V. V. Kondratenko, Y. P. Pershin, S. A. Yulin, E. N. Zubarev, H. A. Padmore, K. C. Cheung, G. E. van Dorssen, M. Roper, L. L. Balakireva, R. V. Serov, and A. V. Vinogradov, "Synthesis and measurement of normal incidence x-ray multilayer mirrors optimized for a photon energy of 390 eV," Nucl. Instrum. Methods Phys. Res. A **345**, 594–603 (1994).
9. D. Sayre, J. Kirz, R. Feder, D. M. Kim, and E. Spiller, "Potential operating region for ultrasoft x-ray microscopy of biological materials," Sciences **196**, 1339 (1977).
10. J. E. Bjorkholm, J. Bokor, L. Eichner, R. R. Freeman, W. M. Mansfield, L. Szeto, D. W. Taylor, D. M. Tennant, O. R. Wood, II, T. E. Jewell, D. L. White, W. K. Waskiewicz, D. L. Windt, and A. A. MacDowell, "Soft x-ray projection lithography," Opt. Photon. News **2** (**5**), 27–30 (1991).
11. A. M. Hawryluk and N. M. Ceglio, "Wavelength considerations in soft-x-ray projection lithography," Appl. Opt. **32**, 7062–7067 (1993).
12. L. Golub, M. Herant, K. Kalata, I. Lovas, G. Nystrom, F. Pardo, E. Spiller, and J. Wilczynski, "Sub-arcsecond observations of the solar x-ray corona," Nature **344**, 842–844 (1990).
13. A. M. Hawryluk, N. M. Ceglio, and D. G. Stearns, "Applications of microfabrication technology to x-ray laser cavities," J. Vac. Sci. Technol. B **6**, 2153–2157 (1988).
14. C. M. Brown, U. Feldman, J. F. Seely, M. C. Richardson, H. Chen, J. H. Underwood, and A. Zigler, "Imaging of laser-produced plasmas at 44 Å using a multilayer mirror," Opt. Commun. **68**, 190–195 (1988).
15. A. K. Ray-Chaudhuri, W. Ng, S. Liang, S. Singh, J. T. Welnak, J. P. Wallace, C. Capasso, F. Cerrina, G. Margaritondo, J. H. Underwood, J. B. Kortright, and C. C. Perrera, "First results of microspectroscopy from a scanning photoemission microscope with a submicron probe size," J. Vac. Sci. Technol. A **11**, 2324–2329 (1993).
16. S. V. Gaponov, S. A. Gusev, Y. Y. Platonov, and N. N. Salashchenko, "Synthetic multilayer reflectors and selectors for the soft x-ray. I. Choice of materials and design of multilayer mirrors," Sov. Phys. Tech. Phys. **29**, 442–445 (1984).
17. P. A. Kearney, J. M. Slaughter, and C. M. Falco, "Materials for multilayer x-ray optics at wavelengths below 100 Å," Opt. Eng. **30**, 1076–1080 (1991).
18. A. E. Rosenbluth, "Computer search for layer materials that maximize the reflectivity of x-ray multilayers," Rev. Phys. Appl. **23**, 1599–1621 (1988).
19. M. Yamamoto and T. Namioka, "Layer-by-layer design method for soft-x-ray multilayers," Appl. Opt. **31**, 1622–1630 (1992).
20. B. L. Henke, E. M. Gullikson, and J. C. Davis, "X-ray interactions: photoabsorption, scattering, transmission, and reflection at $E = 50$–$30{,}000$ eV, $Z = 1$–92," At. Data Nucl. Data Tables **54**, 181–342 (1993).
21. P. A. Kearney, "New materials for multilayer soft x-ray optics for wavelengths below 124 angstrom by sputtering and molecular beam epitaxy," Ph.D. dissertation (University of Arizona, Tucson, Arizona, 1994).
22. C. M. Falco, "Structural and electronic properties of artificial metallic superlattices," J. Phys. **45**, C5-499–C5-507 (1984).
23. C. Montcalm, B. T. Sullivan, H. Pépin, J. A. Dobrowolski, and M. Sutton, "Extreme-ultraviolet Mo/Si multilayer mirrors deposited by radio-frequency-magnetron sputtering," Appl. Opt. **33**, 2057–2068 (1994).
24. See, for example, J. M. Slaughter, D. W. Schulze, C. R. Hills, A. Mirone, R. Stalio, R. N. Watts, C. Tarrio, T. B. Lucatorto, M. Krumrey, P. Mueller, and C. M. Falco, "Structure and performance of Si/Mo multilayer mirrors for the extreme ultraviolet," J. Appl. Phys. **76**, 2144–2156 (1994), and references therein.
25. D. G. Stearns, "The scattering of x-rays from nonideal multilayer structures," J. Appl. Phys. **65**, 491–506 (1989).
26. D. T. Cromer and D. Liberman, "Relativistic calculation of anomalous scattering factors for x rays," J. Chem. Phys. **53**, 1891–1898 (1970).
27. M. S. Bravman and R. Sinclair, "The preparation of cross-sectional specimens for transmission electron microscopy," J. Electron Microsc. Technol. **1**, 53–61 (1984).
28. R. Van Leeuwen, C. D. England, J. R. Dutcher, C. M. Falco, W. R. Bennett, and B. Hillebrands, "Structural and magnetic properties of Ti/Co multilayers," J. Appl. Phys. **67**, 4910–4912 (1990).
29. F. Hong and G. A. Rozgonyi, "Interdiffusion, phase transformation, and epitaxial $CoSi_2$ formation in multilayer Co/Ti–Si(100) system," J. Electrochem. Soc. **141**, 3480–3488 (1994).
30. W. Liu, A. Hu, S. S. Jiang, Y. Qiu, W. H. Liu, and Z. Q. Wu, "An x-ray diffraction study on Cu–Ti metallic multilayers," J. Phys. Condens. Matter **1**, 8771–8778 (1989).
31. P. Børgesen, T. L. Alford, D. A. Lilienfeld, and H. H. Johnson, "Low temperature ion beam mixing of bilayer and multilayers in the Ti–Cu system," Appl. Phys. A **50**, 161–164 (1990).
32. A. Bruson and J. C. Yamegni-Noubeyo, "Atomic diffusion in sinusoidally modulated Cu_xTi_{1-x} amorphous multilayers," Physica Status Solidi A **138**, 199–206 (1993).
33. E. Puppin, V. Krishnamurthy, and C. R. Helms, "Annealing behaviour of refractory metal multilayers on Si: The Mo/Ti and W/Ti systems," J. Appl. Phys. **63**, 2414–2419 (1988).
34. A. I. Fedorenko, V. V. Kondratenko, Y. P. Pershin, O. V. Poltseva, E. N. Zubarev, L. L. Balakireva, V. V. Didyk, and V. V. Burtsev, "Structure and optical properties of multilayer x-ray mirrors for long wave part (3.1–4.4 nm) of water window," Cryst. Res. Technol. **29**, 1139–1147 (1994).
35. C. Sella, M. Mâaza, M. Kaabouchi, S. El Monkade, M. Miloche, and H. Lassri, "Annealing effects on the structure and magnetic properties of Ni/Ti multilayers," J. Magn. Magn. Mater. **121**, 201–204 (1993).
36. O. Elsenhans, P. Boni, H. P. Friedli, H. Grimmer, P. Buffat, K. Leifer, J. Sochtig, and I. S. Anderson, "Development of Ni/Ti multilayer supermirrors for neutron optics," Thin Solid Films **246**, 110–119 (1994).
37. M. Mâaza, B. Farnoux, F. Samuel, C. Sella, F. Wehling, F. Bridou, M. Groos, B. Pardo, and G. Foulet, "Reduction of the interfacial diffusion in Ni–Ti neutron-optics multilayers by carburation of the Ni–Ti interfaces," J. Appl. Crystallogr. **26**, 574–582 (1993).
38. A. F. Jankowski, J. P. Hayes, and P. B. Ramsey, "Interface controlled amorphization of crystalline Ni/Ti multilayers," in *Defect-Interface Interactions*, E. P. Kvam, A. H. King, M. J. Mills, T. D. Sands, and V. Vitek, eds., Vol. 319 of the Materials Research Society Symposium Proceedings (Materials Research Society, Pittsburgh, Pa., 1994), pp. 381–386.
39. T. D. Shen, M. X. Quan, J. T. Wang, and Z. Q. Hu, "Amorphous phase growth by isothermal annealing-induced interdiffusion reactions in mechanically deformed Ni/Ti multilayered composites," J. Mater. Sci. **29**, 2981–2986 (1994).
40. G. E. Winters, K. M. Unruh, C. P. Swann, M. E. Patt, B. E. White, and E. J. Cotts, "Solid-state reactions in multilayer Ni/Ti thin film composites," in *Kinetics of Phase Transformations*, M. O. Thompson, M. J. Aziz, and G. B. Stephenson, eds., Vol. 205 of the Materials Research Society Symposium Proceedings (Materials Research Society, Pittsburgh, Pa., 1992), pp. 215–220.
41. M. Bouhki, A. Bruson, and P. Guilmin, "X-ray diffraction study of amorphization along interfaces in polycrystalline Ni/Ti multilayers," Solid State Commun. **83**, 5–9 (1992).
42. M. A. Hollanders, B. J. Thijsse, and E. J. Mittemeijer, "Amorphization along interfaces and grain boundaries in polycrys-

talline multilayers: an x-ray diffraction study of Ni/Ti multilayers," Phys. Rev. B **42**, 5481–5494 (1990).
43. B. M. Clemens, "Effect of sputtering pressure on the structure and solid-state reaction of titanium–nickel compositionally modulated film," J. Appl. Phys. **61**, 4525–4529 (1987).
44. A. D. Akhsakhalyan, S. V. Gaponov, S. A. Gusev, Y. Y. Platonov, N. N. Salashchenko, and N. I. Polushkin, "Multilayer x-ray mirrors for the wavelength interval 25–44 Å," Sov. Technol. Phys. Lett. **12**, 448–449 (1986).
45. H. Nagata, "Nickel/vanadium and nickel/titanium multilayers for x-ray optics," Jpn. J. Appl. Phys. **29**, 1215–1219 (1990).
46. Y. Horikawa, K. Nagai, and Y. Iketaki, "Soft x-ray reflectometry with a laser-produced plasma source," Opt. Eng. **33**, 1721–1725 (1994).
47. P. A. Kearney, J. M. Slaughter, and C. M. Falco, "Boron-based multilayers for soft x-ray optics," in *Multilayer Optics for Advanced X-Ray Applications*, N. M. Ceglio, ed., Proc. SPIE **1547**, 63–70 (1991).
48. J. M. Slaughter, P. A. Kearney, and C. M. Falco, "Characterization of Pd-B, Ag-B and Si-B interfaces," in *Multilayer Optics for Advanced X-Ray Applications*, N. M. Ceglio, ed., Proc. SPIE **1547**, 71–79 (1991).
49. A. P. Zwicker, S. P. Regan, M. Finkenthal, H. W. Moos, E. B. Saloman, R. Watts, and J. R. Roberts, "Peak reflectivity measurements of W–C, Mo–Si and Mo–B_4C multilayer mirrors in the 8–190-Å range using both $K\alpha$ line and synchrotron radiation," Appl. Opt. **29**, 3694–3698 (1990).
50. A. F. Jankowski and P. L. Perry, "Characterization of Mo/B_4C multilayers," Thin Solid Films **206**, 365–368 (1991).
51. I. A. Kopilets, V. V. Kondratenko, A. I. Fedorenko, E. N. Zubarev, O. V. Poltseva, A. G. Ponomarenko, and I. I. Lyakhovskaya, "Evolution of structure, phase composition and x-ray reflectivity of multilayer mirrors Mo-(B + C) after annealing at 400–1100 °C," in *X-Ray Optics and Surface Science*, A. V. Vinogradov, ed., Proc. SPIE **2453**, 25–32 (1995).
52. C. Montcalm, B. T. Sullivan, M. Ranger, J. M. Slaughter, P. A. Kearney, C. M. Falco, and M. Chaker, "Mo/Y multilayer mirrors for the 8–12-nm wavelength region," Opt. Lett. **19**, 1173–1175 (1994).
53. C. Montcalm, B. T. Sullivan, S. Duguay, M. Ranger, W. Steffens, H. Pépin, and M. Chaker, "In-situ reflectances measurements of soft x-ray/extreme-ultraviolet Mo/Y multilayer mirrors," Opt. Lett. **20**, 1450–1452 (1995).
54. F. R. de Boer, R. Boom, W. C. M. Mattens, A. R. Miedema, and A. K. Niessen, "*Cohesion in metals: transition metal alloys*," Vol. 1 of Cohesion and Structure Series, F. R. de Boer and D. G. Pettifor, eds. (North-Holland, New York, 1988).
55. D. G. Stearns, R. S. Rosen, and S. P. Vernon, "Fabrication of high-reflectance Mo–Si multilayer mirrors by planar-magnetron sputtering," J. Vac. Sci. Technol. A **9**, 2662–2669 (1991).
56. D. L. Windt, R. Hull, and K. Waskiewicz, "Interface imperfections in metal/Si multilayers," J. Appl. Phys. **71**, 2675–2678 (1992).
57. J. A. Thornton, "The microstructure of sputter-deposited coatings," J. Vac. Sci. Technol. A **4**, 3059–3065 (1986).
58. O. Kubaschewski and C. B. Alcock, *Metallurgical Thermochemistry*, 5th ed., Vol. 24 of International Series on Materials Sciences and Technology, G. V. Raynor, ed. (Pergamon, Oxford, 1979), pp. 268–320.
59. D. D. Wagman, W. H. Evans, V. B. Parker, R. H. Schumm, S. M. Bailey, I. Halow, K. L. Churney, and R. L. Nuttall, *CRC Handbook of Chemistry and Physics*, 71st ed. (CRC, Boca Raton, Fla., 1990), pp. 5-16–5-59.
60. P. Boher, L. Hennet, and P. N. Houdy, "Three materials soft x-ray mirrors: theory and application," in *Advanced X-Ray/EUV Radiation Sources and Applications*, J. P. Knauer and G. K. Shenoy, eds., Proc. SPIE **1345**, 198–212 (1990).
61. C. Montcalm, P. A. Kearney, J. M. Slaughter, M. Chaker, and C. M. Falco, "Preliminary survey of material pairs for XUV multilayer mirrors for wavelengths below 130 Å," in *Physics of X-Ray Multilayer Structures*, Vol. 6 of 1994 OSA Technical Digest Series (Optical Society of America, Washington, D.C., 1994), paper MA2.